Simulation of polyethylene glycol and calcium-mediated membrane fusion

Pannuzzo, Martina; De Jong, Djurre H.; Raudino, Antonio; Marrink, Siewert J.

Published in:
Journal of Chemical Physics

DOI:
10.1063/1.4869176

Simulation of polyethylene glycol and calcium-mediated membrane fusion

Martina Pannuzzo, Djurre H. De Jong, Antonio Raudino, and Siewert J. Marrink

Citation: The Journal of Chemical Physics **140**, 124905 (2014); doi: 10.1063/1.4869176
View online: http://dx.doi.org/10.1063/1.4869176
View Table of Contents: http://scitation.aip.org/content/aip/journal/jcp/140/12?ver=pdfcov
Published by the AIP Publishing

Simulation of polyethylene glycol and calcium-mediated membrane fusion

Martina Pannuzzo,[1,a)] Djurre H. De Jong,[2] Antonio Raudino,[3] and Siewert J. Marrink[2]
[1]*Department of Computational Biology, Universität Erlangen-Nürnberg, Staudtstr.5-91058, Erlangen, Germany*
[2]*Groningen Biomolecular Sciences and Biotechnology Institute and Zernike Institute for Advanced Materials, University of Groningen, Nijenborgh 7, 9747 AG Groningen, The Netherlands*
[3]*Dipartimento di Scienze Chimiche, Università di Catania, Viale A. Doria 6-95125, Catania, Italy*

(Received 25 October 2013; accepted 26 February 2014; published online 31 March 2014)

We report on the mechanism of membrane fusion mediated by polyethylene glycol (PEG) and Ca^{2+} by means of a coarse-grained molecular dynamics simulation approach. Our data provide a detailed view on the role of cations and polymer in modulating the interaction between negatively charged apposed membranes. The PEG chains cause a reduction of the inter-lamellar distance and cause an increase in concentration of divalent cations. When thermally driven fluctuations bring the membranes at close contact, a switch from *cis* to *trans* Ca^{2+}-lipid complexes stabilizes a focal contact acting as a nucleation site for further expansion of the adhesion region. Flipping of lipid tails induces subsequent stalk formation. Together, our results provide a molecular explanation for the synergistic effect of Ca^{2+} and PEG on membrane fusion. © *2014 AIP Publishing LLC*. [http://dx.doi.org/10.1063/1.4869176]

INTRODUCTION

Membrane fusion is a ubiquitous and fundamental process in biological systems, e.g., for hormone secretion and vesicle mediated synaptic transmission.[1–3] The importance of multi-valent cations (mainly Ca^{2+}) on fusion *in vivo*[4] and *in vitro*[5] is well known. Adsorbed multi-valent cations may form either *cis* complexes between negative lipids belonging to the same membrane, or *trans* complexes between lipids belonging to opposite membranes.[6] *Trans* complexes appear only when the membrane distance is of the order of the ion diameter, otherwise only *cis* complexes form. Addition of water-soluble polymers, e.g., polyethylene glycol (PEG), that do not appreciably interact with vesicles' surfaces, dramatically enhances the fusion rate.[7] The polymer effect is mainly due to osmotic forces originating from the exclusion of polymer chains from the inter-lamellar spacing. The exclusion is characterized by a combination of steric and electrostatic effects. Recently we showed that the exclusion of the low dielectric permittivity polymer chains forces ions inside the membrane gap leading to an increase of bound cations.[8] Indeed, the presence of both divalent cations and PEG is synergistic on the fusion rate of charged vesicles.[9]

The detailed mechanism of PEG and Ca^{2+} mediated fusion is still unknown. Much of the difficulty can be traced to the involved length and time scales: tens of nanometers and milliseconds. These scales are not easily accessible by direct experimental observation. Particle based computer simulations, in particular coarse-grained molecular dynamics (CGMD), have emerged as an important tool for studying membrane fusion.[10,11] Here we simulate the fusion of two membranes composed of negatively charged 1-palmitoyl-2-oleoyl-sn-glycero-3-phosphoglycerol (POPG) lipids, using the CG Martini model.[12] Mimicking experimental setups, we add both PEG and Ca^{2+} to induce fusion. We compare our results to control simulations in which either, or both, PEG or Ca^{2+} are absent, and to membranes composed of neutral 1,2-dipalmitoyl-sn-glycero-3-phosphocholine (DPPC) lipids.

METHODS

Simulation parameters

All interactions are described by the CG Martini force field,[12] which uses a mapping of on average four heavy atoms to one CG interaction site. The force field has been primarily parameterized to match thermodynamic quantities such as the free energy of hydration, solvation, and partitioning between polar and apolar solvents. In this work, we used the literature parameters for water and sodium/chloride ions,[12] DPPC,[12] POPG,[12] and PEG.[13] POPG consists of 14 interaction sites in Martini. The glycerol headgroup of PG is represented by a neutral, hydrophylic P4 particle and the phosphatidyl group by a Qa particle carrying a negative unit charge. The choline moiety of the PC headgroup is modeled as a positively charged Q0 site. The glycerol backbone is described by two non-polar Na particles. Oleoyl chains are represented by a linear string of 5 apolar beads (C1-C1-C3-C1-C1), palmitoyl chains by strings of four C1 beads. Na^+ and Cl^- are modeled by Qd and Qa particles, with $+e$ and $-e$ charge, respectively, and Ca^{2+} is modeled as a Qd particle with a $+2e$ charge. The polymer PEG is represented by 37 SN0 type particles, with each CG particle representing a single repeat unit. For the full topologies, including bonded terms, see http://cgmartini.nl, where topology files in Gromacs format are readily available. A recent review of the Martini force field can be found in Ref. 14.

a)Authors to whom correspondence should be addressed. Electronic mail: martina.pannuzzo@gmail.com

All simulations were run using version 4.5.5 of Gromacs.[15] Equilibration was performed by using the Berendsen weak coupling thermostat and barostat algorithms[16] with coupling constants of 1.0 ps and 3.0 ps, respectively. After equilibration, the temperature was kept constant at 450 K using the v-rescale algorithm[17] with a time constant of 1.0 ps. The Parrinello-Rahman algorithm[18] was applied for semi-isotropic pressure coupling (1 bar). The equation of motion were integrated using a leap-frog algorithm and a timestep of 20 fs (10 fs in the presence of PEG polymer). Following standard protocol associated with the Martini force field, the LJ and Coulomb potentials were smoothly shifted to zero between 0 and 1.2 and between 0.9 and 1.2 nm, respectively, using the Gromacs shifting function. The neighbor list was updated every 10 steps with a cutoff of 1.4 nm. Electrostatic interactions were screened implicitly (e = 15). The center of mass motion was removed every step. Periodic boundary conditions were applied in all directions.

Testing of Ca^{2+} and PEG models

CG models for ions have to be considered with care, and in particular for Ca^{2+} no parameterization effort has been previously undertaken. To test our Ca^{2+} model, we analyzed the binding mode of the ion with the POPG membrane. The observed binding mode of Ca^{2+} is comparable to predictions based on all-atom models,[19,20] with Ca^{2+} strongly adsorbed at the level of the phosphate groups, on average binding two negatively charged lipids (see Fig. S1 of the supplementary material[38]).

Although the PEG Martini model has been shown[13] to reproduce key properties of the polymer melt, and of single chains in solution, its electro-osmotic properties have not been tested yet. To do so, we simulated ionic solutions of PEG chains. For an electrolyte solution dissolved in a binary solvent, ions induce a phase separation when the ion solvation energy for a specific solvent overcomes the entropy of mixing[21] (low in polymer solutions because of chain connectivity). An initial homogeneous water/polymer mixture thus separates into coexisting fluid phases (so-called salting-out effect). Mean-field theories[8] and experimental data[36,37] show that multi-valent ions are much more effective (about one order of magnitude) than uni-valent ions. As shown in Fig. S2, our CG model is capable of reproducing this effect (see the supplementary material[38]).

System composition and set-up

The following systems were simulated:

(a) Two flat bilayers made up of 5304 negatively charged POPG lipids. The bilayers were inserted in a water box (141917 water beads, representing four times as many real water molecules) in an asymmetrical way in order to create a smaller inter-membrane space and larger external region. The solution also contained 0.02 M calcium ions (340 CG beads) and 10% volume of inert uncharged polymer chains of polyethylene glycol (300 PEG molecules made up of 37 beads, with one bead per monomer). Furthermore, the solution contained 0.05 M sodium chloride (824 sodium ions and 824 chloride ions) plus an additional 4624 sodium counter ions making the solution electroneutral.
(b) The same system as (a) but deprived of calcium ions (with additional sodium ions assuring overall electroneutrality of the system)
(c) The same system as (a) but deprived of PEG.
(d) The same system as (a) but deprived of both PEG and calcium ions.
(e) Similar setup as (a) but with neutral DPPC lipids.

The relative concentration of the different species, in or outside the inter-membrane space in system (a), has been determined from previous simulations described in Ref. 8. Here the system consisted of two membranes, separated by 5 nm and having free borders along the y-axis in order to allow for a flux of ions and PEG in and out of the inter-membrane space (Fig. 1(A)). After equilibrating the system for 500 ns, while constraining the lipids' centers of masses, the density profiles of the species (ions and polymer) appeared stabilized. In particular, the inter-membrane region is depleted of PEG (Fig. 1(B)). Details about the forces involved in the polymer exclusion are discussed in Ref. 8. The system was then resized in order to have infinite, periodic membranes in the x and y dimensions and constraints were released to allow fluctuations. Residual PEG polymer chains that were in the inter-bilayer space were removed to facilitate the fusion process (Fig 1(C)). For systems (b)–(e), excess PEG or Ca^{2+} was simply removed from the system. The alchemical change from POPG to DPPC involved removal of the terminal tail bead from the oleoyl chain. Thus starting structures were generated for all the simulations described in the current paper. Finally, three replicas of each system were simulated for 1.0 μs, starting from random initial velocities. Initially, simulations were run at

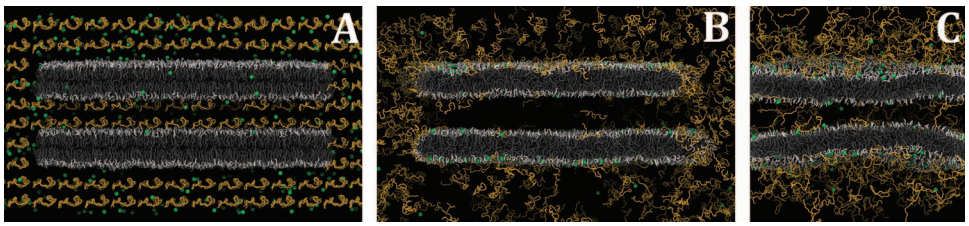

FIG. 1. System set-up. (A) Starting structure with ions and polymer uniformly distributed. Lipid tails are depicted in grey, headgroups are shown in white, calcium ions in green, and polymer in yellow. Water is not depicted. (B) Structure after equilibration phase with polymer depleted and Ca^{2+} enriched in inter-lamellar space. (C) The system after removal of the free boundaries and inter-bilayer PEG chains, i.e., the starting structure for the current set of simulations.

physiological temperature (300 K); however, no close apposition of the membranes on the accessible microsecond time scale was observed. To increase the magnitude of the membrane undulations, required to bring the apposed membranes in close contact, the temperature was raised to 450 K. Note, due to periodic boundary conditions, the simulated membrane patches remain stable even at 450 K. Apart from a slight increase in area/lipid (about 10% compared to physiological temperatures), no destabilization occurs. A set of additional simulations was performed on systems in which the inter-membrane distance was manually decreased to 2–3 nm, and with varying concentrations of ions. These simulations were performed at a reduced temperature of 300–350 K, and run for 5 μs.

Reverse transformation

To provide an atomistically detailed view on the calcium induced *trans*-bridges, we reverse transformed a representative configuration from our CG ensemble. Reverse transformation was done using the implementation by Rzepiela *et al.*[22] Parameters for the atomistic lipid were taken from a library of pure lipid bilayers[23] consistent with the Gromos 53a6 force field. The reverse transformation simulations consisted of 10 000 steps of simulated annealing, using a time step of 2 fs, in which the system was gradually cooled from 1000 K to 298 K.

Analysis details

The mean inter-membrane distance is calculated as the distance between the center of mass of lipid headgroups (P-P) in each of the monolayers facing the inter-membrane space, using the Gromacs tool g_dist. Frames were analyzed every 1 ns. Contacts between Ca^{2+} ions and the phosphate group of the lipid headgroups were calculated using the Gromacs tool g_hbond, using a cutoff of 0.7 nm (corresponding to the position of the 1st minimum of the radial distribution function). We consider calcium ions *trans* bonded to lipid headgroups whenever calcium ions adsorbed to one leaflet are simultaneously in contact with the opposite one. For contacts with the opposite bilayer a slightly smaller cutoff of 0.5 nm was used to avoid counting transient contacts. Contacts between tails of the apposed membranes were based on the contact between the mid tail beads, using a cutoff of 0.5 nm.

RESULTS

Our starting configuration is a system of two membranes separated by a water layer of approximately 5 nm and depleted of PEG chains but enriched in Ca^{2+} (Fig. 1(C)). The relative concentrations of the different species in or outside the inter-membrane space have been determined from previous simulations[8] in which free boundaries, present during the equilibration phase, allowed exchange of PEG and Ca^{2+} (see Methods). From this starting point, we observe formation of an adhesion site within 100 ns of simulation (Fig 2(A)). This contact zone is stable for a few 100 ns, and then a stalk is formed connecting the *trans* monolayers at the onset of fusion (Fig 2(B)). Full fusion (i.e., opening of a fusion pore) is not observed and likely would require tension.[24] The same event was observed in three independent simulations, with stalks appearing on a 200–900 ns time scale (see Fig. S3 of the supplementary material[38]). Note that we have used an elevated temperature (450 K) to increase the likelihood of forming the necessary initial contacts between the freely undulating membranes (see the Methods). Importantly, once contact formation has been established, a decrease of the temperature to 300 K shows stalk formation to proceed via the same pathway as described above (see Fig. S4 of the supplementary material[38]).

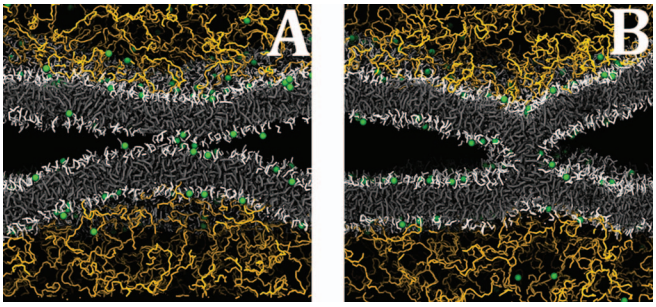

FIG. 2. Stalk formation induced by PEG and Ca^{2+}. (A) Extended adhesion site stabilized by *trans* complexes, at 400 ns. Lipid tails are depicted in grey, headgroups are shown in white, calcium ions in green, and polymer in yellow. Water is not depicted. (B) Final state of the system after 1.0 μs, characterized by a stalk connecting the contacting monolayers.

The role of calcium is illustrated by looking at the time evolution of the number of *trans* complexes, as depicted in Fig. 3(A). Initially, only *cis* complexes exist. This is followed by a transition of calcium bridges from *cis* to *trans* conformation, resulting in a transition from a weak long-distance adhesion to a tight short-distance bound state stabilized by *trans* bridges. The amount of *trans* complexes fluctuates between 15–20, and occurs over the entire membrane area. Figure 3(B) shows a close up view of a typical *trans* complex, in full atomic detail obtained after a backmapping procedure (see the Methods). The calcium ion bridges multiple negatively charged lipids from the opposing membranes. Similar bridges were observed previously in all-atom simulations,[25] but initiation of fusion could not be observed. On the extended time scale accessible by our CG approach, we see that the bridging calcium ions locally initiate flipping of lipid tails (Fig. 3(C)). This is a stochastic event, accounting for the range of time scales we observe in our replicate simulations. Once lipid flipping is initiated, formation of the stalk is irreversible.

A number of control simulations were performed to test whether or not the fast fusion is indeed due to the combined presence of PEG and Ca^{2+}. Control systems were depleted in calcium or polymer, or both, and simulated for 1.0 μs from the same initial state. In all cases, fusion was not observed. Figure S5(a) of the supplementary material[38] shows snapshots of the POPG system in presence of PEG, but lacking Ca^{2+}. The membranes fluctuate, but do not form stable contacts. The same behavior is observed when POPG is replaced by DPPC (see Fig. S5(b) of the supplementary material[38]). In agreement with the experimental findings,[7] neutral membranes of pure DPPC never form an adhesion site,

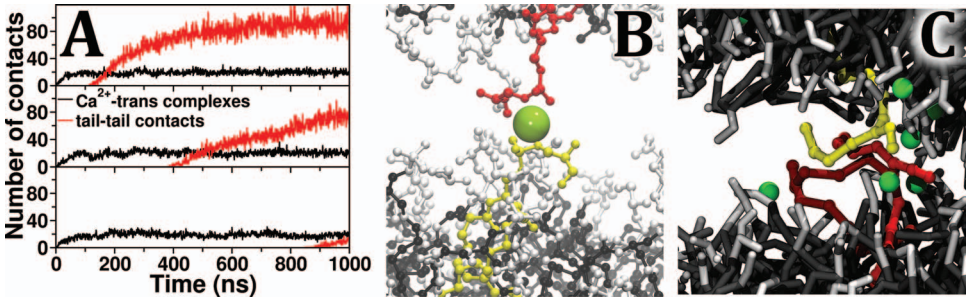

FIG. 3. Fusion triggered by formation of *trans* Ca^{2+} bridges. (A) Formation of *trans* bridges along time. The black profile shows the number of contacts between calcium ions absorbed to one bilayer with the lipid headgroups belonging to the opposite bilayer. The red profile shows the number of contacts between tails of the two bilayers. Individual traces from three independent simulations are reported. (B) Zoomed view showing a *trans* contact site where a calcium ion (green) promotes the interactions between lipids (red/yellow) belonging to opposite bilayers. Atomistic representation obtained by reverse mapping the CG system. (C) Lipid flipping at the adhesion site, induced by a *trans* contact. The two lipids that first flip between the apposed membranes are depicted in red and yellow, calcium ions at close proximity in green.

even in presence of PEG and Ca^{2+}. For a more quantitative assessment, we measure the closest distance of approach between the apposed membranes, shown as function of time in Fig. S5(c) (see the supplementary material[38]). Clearly, the contemporary presence of PEG and calcium induces a smaller mean inter-membrane distance in comparison to systems containing only PEG or Ca^{2+} or neither, or lacking the ability to strongly bind calcium (DPPC).

Taken together, our results suggest that PEG generates a reduced inter-membrane distance guaranteeing smaller waiting time for fusion, and, in addition, mediates higher inter-membrane concentrations of Ca^{2+}. In turn, Ca^{2+} is the factor driving fusion. To substantiate the effect of calcium ions on the adhesion/fusion rate, we performed several additional simulations without PEG and with a preset, smaller, inter-lamellar distance. The distance between the two POPG membranes was varied from 2 to 3 nm, exploring different concentrations of Ca^{2+} in the interlamellar space (0.0, 0.01, 0.05 M) and varying temperature (300, 350, and 450 K). The results are summarized in Table I. At the lowest temperature (300 K), fusion is only observed at a small interlamellar distance (2 nm) and high Ca^{2+} concentration (0.05 M). At lower Ca^{2+} concentrations, spontaneous fusion only occurs at elevated temperature (350 K). Replacing Ca^{2+} with Na^{+} does not lead to stalk formation. With a larger initial distance (3 nm), Ca^{2+} induced fusion is still observed, but again requires an elevated temperature (350 K at 0.05 M, or 450 K at 0.01 M). With DPPC, stable adhesion is never reached.

TABLE I. Effect of Ca^{2+} on membrane adhesion/fusion. Comparison of 5 μs simulations with different initial interlamellar distances (d), temperatures (T), and salt concentrations.

Membrane	NaCl (M)	$CaCl_2$ (M)	PEG	d (nm)	T (K)	Adhesion	Stalk
POPG	0.1	No	No	2	350	No	No
POPG	0.1	0.01	No	2	350	Yes	No
POPG	0.06	0.05	No	2	350	Yes	Yes
POPG	0.06	0.05	No	3	350	Yes	Yes
POPG	0.06	0.05	No	2	300	Yes	Yes
POPG	0.1	0.01	No	3	350	Yes	No
POPG	0.1	0.01	No	3	450	Yes	Yes
DPPC	0.1	0.01	No	2	350	No	No

DISCUSSION

Based on the current data and our previous findings,[8,26,27] we propose a multiple stage mechanism for PEG/Ca^{2+} mediated fusion, starting from bilayer approach, via adhesion, to stalk formation. Each of these steps is discussed in the following.

(i) *Bilayer approach*: Exclusion of PEG and concomitant enrichment of Ca^{2+} in the inter-lamellar space results in a decrease of the inter-membrane distance. Since the approach of the bilayers is the key initial step in the fusion pathway, the polymer-induced lowering of the inter-membrane distance suggests a higher fusion rate. This is in agreement with experimental results[28] reporting a variation of the fusion rate with the distance (measured by X-ray and externally tuned by depletion forces). The same is observed here, with a clearly reduced fusion propensity at larger membrane separation (cf. Table I). Furthermore, polymer exclusion from the inter-membrane space is enhanced in case of charged membranes. If we consider two negatively charged membranes embedded in a polyelectrolyte solution, ions tend to accumulate into the interlamellar space to shield the electrostatic repulsion between membranes, promoting the exclusion of polymer (salting-out mechanism). As a consequence of the electro-osmotic release of polymer, negatively charged membranes feel each other at longer distances than neutral membranes, as hypothesized by some authors on the basis of experimental evidence[29,30] and proved by us by electrostatic modelling and MD simulations.[8] This mechanism explains why, in the current set of simulations, either neutral DPPC membranes in presence of PEG alone, or negatively charged POPG membranes without Ca^{2+}, do not reach a stable adhesion state.

(ii) *Adhesion*: Our simulations show that calcium ions are a key component in the stabilization of the adhesion state. Their strong binding to anionic lipids results in *trans*-complex formation, bridging lipids from the closely apposed membranes. Interestingly, a similar mode of action was observed in recent simulations[31] of multi-lamellar membranes in presence of a small cationic peptide. Like

Ca^{2+}, the peptide was able to bridge lipids from opposite leaflets and induce stalk formation. On the other hand, monovalent ions such as Na^{+} are less capable of binding multiple lipids and are therefore unable to induce membrane adhesion. The increased fusion capacity of calcium ions over monovalent ions is corroborated by a large body of experimental studies.[32]

(iii) *Stalk formation*: The onset of stalk formation requires flipping of lipid tails between the apposed membranes. Formation of this local contact site is the main barrier in the initial fusion event, as demonstrated in a number of previous simulation studies.[33,34] Calcium ions trigger this event by constricting the lipid headgroups in a partially dehydrated state. Lipid tails sense the increased hydrophobicity at the interface, thereby increasing the likelihood of tail flipping. Recent all-atom simulations on calcium mediated fusion between micelles support this mechanism.[35] Our simulations furthermore show that once a contact site is formed, it irreversibly expands into a stalk. Further expansion of the stalk into a hemifusion or full fusion state depends on lipid composition and presence of tension/curvature in the system, and was not observed in our simulations.

Future work using more detailed, atomistic, models is required to test these hypotheses that are based on the use of the coarse-grain Martini model. Although properties of lipid membranes are generally well described by this model,[14] the parameterization of ions, in particular Ca^{2+}, has been done at a rather qualitative level mainly due to lack of suitable experimental targets. An accurate description of the interplay between ions and membranes remains a challenge even for fine-grain models. Importantly, the binding mode of Ca^{2+} to phospholipids in our CG model is similar as compared to atomistic models (see Fig. S1 of the supplementary material[38]). It is also reassuring that the back transformation of the *trans* contact to full atomistic detail (Fig. 3(B)) retains the same configuration. With regards to the PEG model, one may question the ability of a CG model to reproduce electro-osmotic effects in a realistic way. To that end, we compared simulations of PEG solutions in the presence of either sodium or calcium chloride, and found a strong salting-out effect in case of divalent cations (see Fig. S2 of the supplementary material[38]). These results are consistent with mean-field calculations[8] and experimental measurements that unambiguously show how multivalent cations are more effective than the monovalent ones.[36,37] Another point of concern is the elevated temperature we used to speed up the kinetics of contact formation and subsequent fusion. We did, however, observe a very similar fusion pathway upon lowering the temperature to 300 K, once the initial contact zone had been established. In addition, we observe calcium-mediated fusion at 300 K between membranes pre-apposed at smaller membrane distances. We are therefore confident that the results presented are relevant also under physiological conditions, although the time scales involved may well be (very) different.

In summary, we show that rapid fusion requires both Ca^{2+} and PEG in agreement with experimental results.[7] A likely mechanism making PEG/Ca^{2+} so efficient in inducing membrane adhesion/fusion may be related to the increased concentration of divalent cations together with a reduction of the inter-lamellar distance. When thermally driven fluctuations bring membranes at close contact, the switch from *cis* to *trans* Ca^{2+} complexes stabilizes a focal contact acting as a nucleation site for further expansion of the adhesion region and subsequent stalk formation.

ACKNOWLEDGMENTS

We thank SARA (Amsterdam, the Netherlands) for computational resources.

[1] W. Wickner and R. Schekman, Nat. Struct. Mol. Biol. **15**, 658 (2008).
[2] S. Martens and H. T. McMahon, Nat. Rev. Mol. Cell. Biol. **9**, 543 (2008).
[3] L. V. Chernomordik and M. M. Kozlov, Nat. Struct. Mol. Biol. **15**, 675 (2008).
[4] J. C. Hay, EMBO Rep. **8**, 236 (2007).
[5] P. K. Tarafdar, H. Chakraborty, S. M. Dennison, and B. R. Lentz, Biophys. J. **103**, 1880 (2012).
[6] A. Portis, C. Newton, W. Pangborn, and D. Papahadjopoulos, Biochemistry **18**, 780 (1979).
[7] B. R. Lentz, Eur. Biophys. J. **36**, 315 (2007).
[8] A. Raudino, M. Pannuzzo, and M. Karttunen, J. Chem. Phys. **136**, 055101 (2012).
[9] W. Guo, P. J. Photos, and T. K. Vanderlick, Ind. Eng. Chem. Res. **45**, 5512 (2006).
[10] A. J. Markvoort and S. J. Marrink, Curr. Top. Membr. **68**, 259 (2011).
[11] H. Ingolfsson, C. A. Lopez, J. J. Uusitalo, D. H. De Jong, S. Gopal, X. Periole, and S. J. Marrink, "The power of coarse-graining in biomolecular simulations," WIREs Comput. Mol. Sci. (published online).
[12] S. J. Marrink, H. J. Risselada, S. Yefimov, D. P. Tieleman, and A. H. De Vries, J. Phys. Chem. B. **111**, 7812 (2007).
[13] H. Lee, A. H. de Vries, S. J. Marrink, and R. W. Pastor, J. Phys. Chem. B. **113**, 13186 (2009).
[14] S. J. Marrink and D. P. Tieleman, Chem. Soc. Rev. **42**, 6801 (2013).
[15] B. Hess, C. Kutzner, D. van der Spoel, and E. Lindahl, J. Chem. Theory Comput. **4**, 435 (2008).
[16] H. J. C. Berendsen, J. P. M. Postma, W. F. van Gunsteren, A. DiNola, and J. R. Haak, J. Chem. Phys. **81**, 3684 (1984).
[17] G. Bussi, D. Donadio, and M. Parrinello, J. Chem. Phys. **126**, 014101 (2007).
[18] M. Parrinello and J. Rahman, J. Appl. Phys. **52**, 7182 (1981).
[19] Y. Mao, Y. Du, X. Cang, J. Wang, Z. Chen, H. Yang, and H. Jiang, J. Phys. Chem. B. **117**, 850 (2013).
[20] A. Martın-Molina, C. Rodrıguez-Beas, and J. Faraudo, Biophys J. **102**, 2095 (2012).
[21] J. Schindler and H. G. Nothwang, Proteomics **6**, 5409 (2006).
[22] A. J. Rzepiela, L. V. Schäfer, N. Goga, H. J. Risselada, A. H. de Vries, and S. J. Marrink, J. Comput. Chem. **31**, 1333 (2010).
[23] A. Kukol, J. Chem. Theory Comput. **5**, 615 (2009).
[24] A. Grafmüller, J. Shillcock, and R. Lipowsky, Phys. Rev. Lett. **98**, 218101 (2007).
[25] Z. K. Issa, C. W. Manke, B. P. Jena, and J. J. Potoff, J. Phys. Chem. B **114**, 13249 (2010).
[26] A. Raudino and M. Pannuzzo, J. Chem. Phys. **132**, 045103 (2010).
[27] A. Raudino, S. J. Marrink, and M. Pannuzzo, J. Chem. Phys. **138**, 234901 (2013).
[28] S. W. Burgess, T. J. McIntosh, and B. R. Lentz, Biochemistry **31**, 2653 (1992).
[29] K. Arnold, O. Zschoering, D. Barthel, and W. Herold, Biochim. Biophys. Acta **1022**, 303–310 (1990).
[30] J. Y. Lehtonen and P. K. Kinnunen, Biophys. J. **68**, 525–535 (1995).
[31] G. Moiset, A. D. Cirac, M. C. A. Stuart, S. J. Marrink, and D. Sengupta, PLoS One **8**, e61541 (2013).
[32] K. Arnold, *Handbook of Biological Physics*, edited by R. Lipowsky and E. Sackmann (Elsevier, Amsterdam, 1995), pp. 903–957.
[33] Y. G. Smirnova, S. J. Marrink, R. Lipowsky, and V. Knecht, J. Am. Chem. Soc. **132**, 6710 (2010).

[34]D. Mirjanian, A. N. Dickey, J. H. Hoh, T. B. Woolf, and M. J. Stevens, J. Phys. Chem. B. **114**, 11061 (2010).
[35]H. H. G. Tsai, W. F. Juang, C. M. Chang, T. Y. Hou, and J. B. Lee, Biochim. Biophys. Acta: Biomembranes **1828**, 2729–2734 (2013).
[36]M. J. Hey, D. P. Jackson, and H. Yan, Polymer **46**, 2567 (2005).
[37]P. Thiyagarajan, D. J. Chaiko, and R. P. Hjelm, Macromolecules **28**, 7730 (1995).
[38]See supplementary material at http://dx.doi.org/10.1063/1.4869176 for the computational methods in detail and the reported results of performed control simulations.